Biointerface Research in Applied Chemistry
Open-Access Journal (ISSN: 2069-5837)

Article
Volume 13, Issue 3, 2023, 256
https://doi.org/10.33263/BRIAC133.256

Influence of Zn^{+2} Doping on Dielectric Properties of Ba-Based Nanoferrites

A. H. AL-Hammadi [1], Sadiq. H. Khoreem [1,2,*]

[1] Physics Department, Faculty of Science, Sana'a University, Sana'a, Yemen
[2] Dept. of Optometry and Vision Science, Faculty of Medical Sciences, Al-Razi University, Sana'a, Yemen
* Correspondence: khoreems@yahoo.com (S.H.K.);

Scopus Author ID 57571836200
Received: 11.03.2022; Accepted: 13.04.2022; Published: 10.06.2022

Abstract: The effect of frequency, temperature, and composition on the dielectric behavior for the composition of $BaNi_{2-x}Zn_xFe_{16}O_{27}$ ferrite samples were studied (with x = 0, 0.4, and 1.6) prepared using the usual ceramic method. The experimental results indicated that the dielectric constant ε′ and dielectric loss ε"decrease as the frequency increases, and increases with increasing temperature. The experimental results indicated that the dielectric constantε′ and dielectric loss ε′′ decreases. The dielectric constant has high values and shows relaxation processes at relatively higher temperatures. The dielectric abnormal behavior of the dielectric constant was observed to shift to lower values as the temperature increases. The dielectric loss tangent initially decreases rapidly with increasing frequency, and increasing tan δ with increasing temperature is attributed to thermal activation of electron transport, responsible for dielectric behavior. The ε′,ε′′ and tanσ were composition-dependent, both decreasing as Zn ion substitution increases.

Keywords: barium nano ferrites; dielectric constant; dielectric loss tangent.

1. Introduction

The nano ferrites continue to be the most important and attractive materials up to becoming a vital source in all life fields from electronics to microwave and radio frequencies. As important, their unique physical characteristic properties, such as dielectric constant, electrical conductivity, and magneto-dielectric properties, play an important role in the electronic industry field. Because of their high uniaxial anisotropy, cost-effectiveness, and high coercive Force, it was used in microwave devices as permanent magnets [1]. The magnetic properties of $BaCo_{2-x}Ni_xFe_{16}O_{27}$ W-type $BaCo_{2-x}Zn_xFe_{16}O_{27}$ - Co-Ni substituted $BaMg_2Fe_{16}O_{27}$ [2-4]. Also, the AC conductivity and dielectric properties of and dielectric behavior for $BaCo_{2-x}Zn_xFe_{16}O_{27}$ W-type $BaCo_{2-x}Cu_xFe_{16}O_{27}$- $BaCo_{2-x}Ni_xFe_{16}O_{27}$- $BaNi_{2-x}Zn_xFe_{16}O_{27}$, and $BaCo_{2-x}Zn_xFe_{16}O_{27}$ W-type hexaferrite [5–8]. To understand the dielectric behaviors and explain the mechanisms of electric conduction in the ferrite, one must study the effect of temperature, composition, and frequency on dielectric and the a.c. electrical conductivity will offer great valuable value information about this behavior. From the dielectric measurement analysis, two elementary electrical characteristics of materials can be examined. The physical phenomenon (conduction nature) represents its ability to transfer electrical charge, and the electrical phenomenon (capacitive) insulating nature, represents its ability to store electrical charge [9]. Therefore, analysis of the dielectric analysis ends up offering the

dielectric constant (ε') and dielectric loss (ε") of a material. Therefore, the present work aimed to study the effects of Zn ions dopant on the dielectric properties for $BaNi_{2-x}Zn_xFe_{16}O_{27}$ W-type hexagonal ferrites as a function of frequency and temperature.

2. Materials and Methods

Highly pure $BaCO_3$, MgO, ZnO, and Fe_2O_3 to produce a sequence of polycrystalline w-type hexagonal nano ferrites in the correct ratio with compositional formula $BaNi_{2-x}Zn_xFe_{16}O_{27}$ (Where x = 0:0, 0.4, and 1.6) by the standard ceramic method. First, the mixed oxides were ground using an electrical agate mortar for 10 h. The powders were then presintered in the air for 20 hours at 900 K degrees Celsius in a furnace. The granules were brought to room temperature gradually. The grinding process was repeated; afterward, the mixtures were pressed into discs, and toroid's under the constant pressure of 29.4×10^7 N/m^2. The discs and toroid's were sintered at 1470 K for 6 hours before being cooled to ambient temperature. The disks were finally sintered in air at 1250 K for 6h and left to be slowly cooled to room temperature within 24 h. As a good contact material for electrical tests, the samples were polished and covered with a thin layer of silver paste. The dielectric was measured under vacuum at different temperatures and frequencies using the complex impedance measuring technique (Lock-in amplifier Stanford SR 510 type, USA). The dielectric constant and loss tangent are calculated by the flowing relation

$\varepsilon_r = \frac{\varepsilon}{\varepsilon_\circ} = \frac{C_d}{C_A}$ (1) $\tan\sigma_e = \frac{\varepsilon''}{\varepsilon'}$ (2) where ε'' s is the imaginary part of the dielectric constant

3. Results and Discussion

3.1. Dielectric constant ε'.

3.1.1. Temperature dependence of dielectric constant ε'.

Figure 1.(a)–(c) depicts the variation of the real part of the dielectric constant (ε') behaviors with frequency for $BaNi_{2-x}Zn_xFe_{16}O_{27}$ ferrite compositions at various temperatures. It can be shown that the dielectric constant ε' has a high value at low frequencies, then drop monotonically with rising frequency and also increases with increasing temperatures at low frequencies. This indicates that charge carriers respond to an externally provided electric field at low frequencies faster, resulting in a higher value of ε′. Charge carriers cannot follow rapid changes in the applied electric field at higher frequencies, resulting in low values of ε′.

The decrease in ε′ with frequency is because, at low frequencies, ε'' for polar materials is explained by the contribution of many polarizability components, namely deformational, electronic, and ionic polarization, as well as relaxation, orientational, and interfacial polarization.

It's worth noting that the high value of ε′ comes primarily from Koop's theory [10]. According to this theory, charge carriers encounter a different resistance as they hop across the grain boundary due to the high charge concentration at the dividing boundaries, resulting in interfacial polarization. As a result, the value of ε′ was increased significantly [11,12]. Peaks on the ε' curves were detected as the temperature increased. This is the abnormal dielectric behavior that had previously been observed [13,14]. The position of the observed peaks was discovered to be dependent on the composition and temperature, with the peaks shifting

towards higher frequencies as the temperature rises and toward lower temperatures as the zinc concentration decreases.

The presence of a collective contribution of two types of charge carriers (p-type and n-type) to the polarization, according to the Rezlescu model, can explain the aberrant behavior of the dielectric constant with frequency and temperature. Because the contribution of p-carriers to polarization is lower and in the opposite direction than that of n-carriers, and because the mobility of p-carriers is lower than that of n-carriers, and their contribution to polarization decreases rapidly at lower frequencies, the contributions of each type of charge carrier to polarization can be added up to give a polarization like Rezlescu [15]. With rising zinc-ions concentration, the maximum in dielectric constant ε′ shifts towards lower frequencies with frequencies and temperature.

3.1.2. Frequency dependence of dielectric constant ε'.

The dielectric constant ε' as a function of temperature for all samples at various frequencies is shown in figure 1.(d)–(f). The dielectric constant ε' increases with increasing temperature until it reaches a maximum value at a specific temperature, after which it begins to decline with increasing temperature quickly. It is clear from figure.1.(d)–(f). that the dielectric constant ε' increases as the temperature rises.

This can be attributed to the fact that dipoles cannot orient themselves with variable electric fields at low temperatures because orientational polarization is linked to the thermal motion of the molecules. It is found nearly constant at low temperatures [16,17]. The dipoles' orientation was changed with increasing temperature, which caused an increase in the value of orientational polarization, which eventually increased the dielectric constant ε' with temperature. To put it another way, the increase in ε′ values with temperature is due to the charge carriers' contribution to polarization. Due to the dipoles' inability to rotate quickly enough at low temperatures, polarization is weak, and they wobble behind the field. The bound charge carriers receive enough thermal excitation energy as the temperature rises to improve polarization, increasing the dielectric constant.

3.2. Dielectric Loss ε″.

3.2.1. Temperature dependence of dielectric loss ε″.

Figure 2.(a)-(c) illustrates the frequency dependence of dielectric loss (ε") for all samples at different temperatures. The dielectric losses (ε") decrease rapidly at low frequencies, then decrease monotonically with increasing frequency until reaching a constant value at a higher frequency. The decreases in dielectric loss as frequency rises can be explained by the fact that at high frequencies, ion vibration may be the only source of dielectric loss; hence ε" has the smallest value. In other words, as the frequency of the applied field surpassed the relaxation frequency, the polarization response became increasingly delayed. Because of the grain boundaries, the resistivity was high at lower frequencies. The energy loss increased in the lower frequency range because the electron exchange between ions (Fe^{3+} and Fe^{2+}) required more energy [18,19]. Because of the high values of dielectric loss ε" [20], the examined samples can be used for microwave radiation absorption and attenuating electromagnetic interference applications.

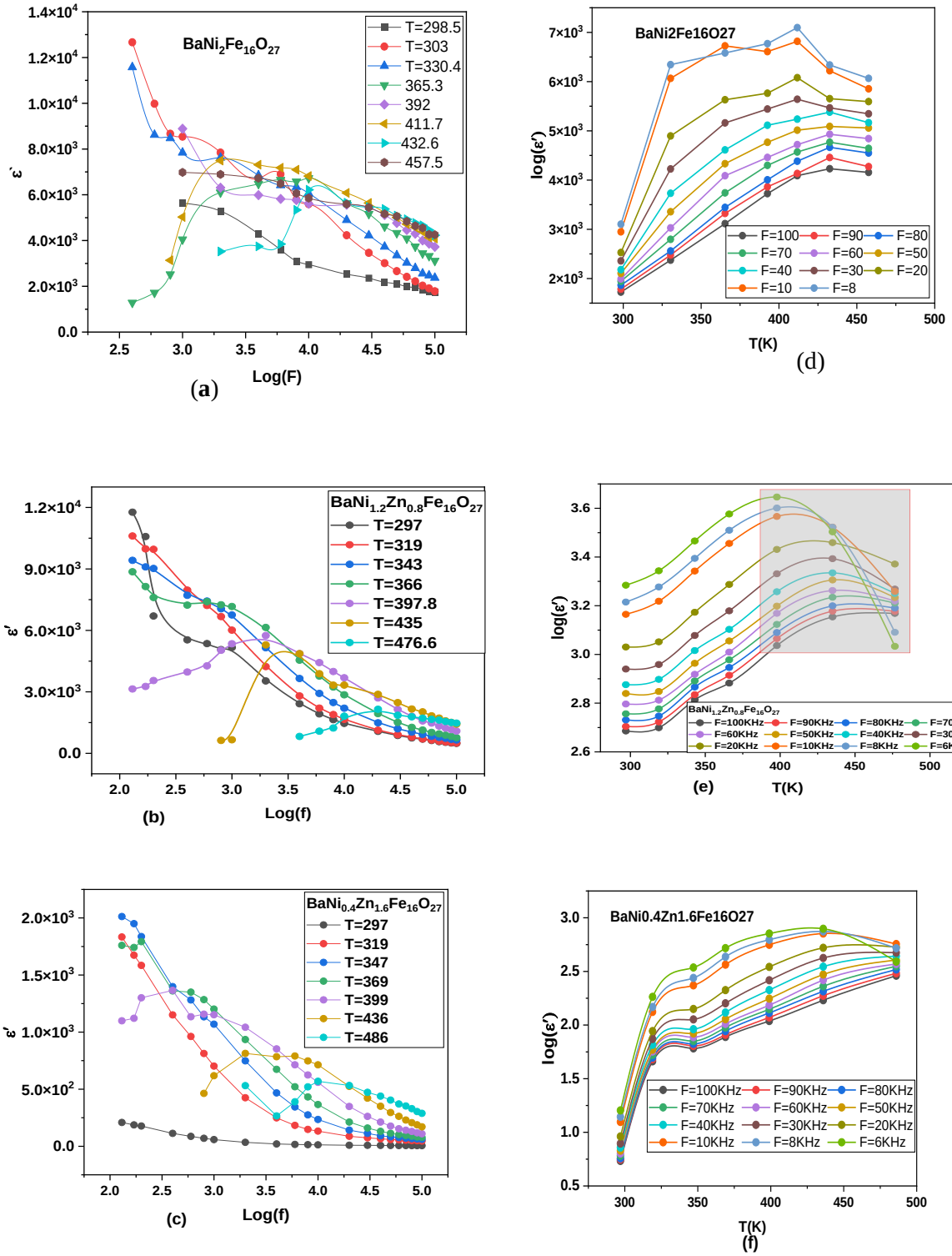

Figure 1. (a, b, c) Dielectric constant vs. frequency of $BaNi_{2-x}Zn_xFe_{16}O_{27}$ (x=0, 1.6 ,0.8) at different temperatures; (d, e, f) Temperature dependence of the dielectric constant (ε′) of $BaNi_{2-x}Zn_xFe_{16}O_{27}$ (x=0, 1.6 ,0.8) at selected frequencies.

3.2.2. Frequency dependence of dielectric loss ε′′.

Dielectric loss is a term used to describe the loss of dielectric properties. Figure 2.(d)-(f). shows the dielectric loss ε“as a function of temperature for all samples at various frequencies. It has been pointed out that increases dielectric loss ε“as the temperature rises. Conduction losses, dipole losses, and vibrational losses are the three types of dielectric losses

[15]. Because conduction losses are proportional to $\sigma_{ac}(\omega)$, they are smallest at low temperatures. Ion migration over long distances necessitates conduction loss. When ions travel, they transfer some of their energy to the lattice in the form of heat. Conduction loss increases as the temperature rises because ac rises with it. As a result ε‘‘, rises as the temperature rises. For many nonlinear optical materials and their applications in devices, a low dielectric constant and high-frequency dielectric loss suggest that the sample has enhanced optical quality with fewer faults, which is crucial.

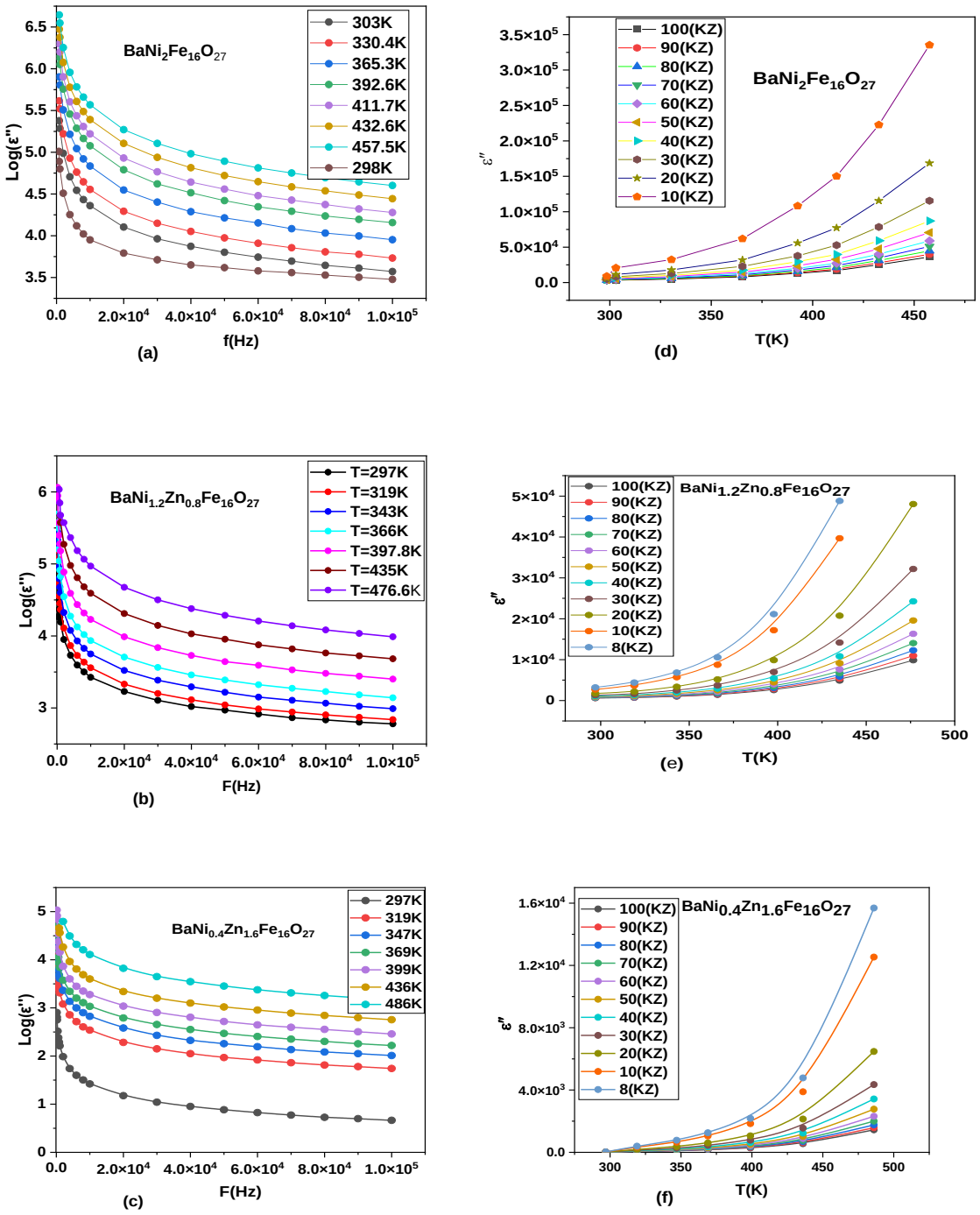

Figure 2. (a, b, c) Dielectric loss vs. frequency of $BaNi_{2-x}Zn_xFe_{16}O_{27}$ (x=0, 0.8 and 1.6) at different temperatures; (d, e, f) Temperature dependence of dielectric loss (ε′‘) with Frequencies.

3.3. Loss tangent (tan σ).

3.3.1. Temperature dependence of loss tangent (tan σ).

The loss tangent (tan δ) as a function of frequency for all the samples is shown in figure.3.(a)-(c). As frequency increases, the dielectric loss tangent falls rapidly, demonstrating dispersion at lower frequencies before becoming fairly constant at higher frequencies. The Maxwell-Wagner model [21,22] and Koop's phenomenological theory [23] are related to these characteristics for dielectric loss in ferrite. Two mechanisms cause ferrite dielectric loss: electron hopping and loaded dipoles defect. The dielectric loss was caused by the low-frequency band. The main cause of dielectric loss in the high-frequency area was the reaction of defect dipoles to the applied field. Due to a shift in the cation state, such as Fe^{3+} - Fe^{2+}, a ferrite dipole was generated during the heat treatment process. In the high-frequency region, the relaxation of dipoles in an electric field reduced as dielectric loss increased [24]. Impurities in the crystal structure and defects in the crystal lattice caused the dielectric loss in the applied field [25]. The dielectric loss tangent is also affected by the sample's structure and sintering temperatures, such as stoichiometry, Fe^{2+} concentration, and structural homogeneity [26]. At low temperatures, it can be shown that tanσ decreases monotonically with increasing frequency, with no peaks. While at high temperatures, the decrease in tanσ at low frequencies is faster than that at high frequencies for all samples, at high temperatures, the decrease in tan at low frequencies is faster than that at high frequencies. At high temperatures, there is also an apparent shoulder on the tanσ curves for the sample with increasing Zinc. As the temperature rises, the position of the peak shifts to higher frequencies. In addition, at all frequencies and for all samples, tan increases with rising temperature.

3.3.2. Frequency dependence of loss tangent (tan σ).

At various temperatures, Figure 3.(d)-(f) shows the frequency dependence of loss tangent tanσ for all samples. It is noticed that dielectric relaxation processes behave normally. The thermal activation of electron transport, which is responsible for dielectric behavior, is responsible for the increase in tanσ with rising temperature. Simultaneously, the variation of dielectric loss with temperature has the same nature as the change of dielectric constant with temperature and can be explained in the same way that the dielectric constant can be explained. It has been discovered that as the temperature rises, so does the dielectric loss. Charge carrier mobility increases as temperature rises, leading to greater polarization and significant dielectric loss. Charge accumulation at grain boundaries causes the observed increased value of the dielectric loss at high temperatures. Temperature causes charge carrier mobility to increase, resulting in increased polarization and high dielectric loss. The observed higher value of the dielectric loss at high temperature is due to charge accumulation at grain boundaries. [27]. At room temperature, the loss tangent tan is very small, but it rapidly increases as the temperature rises; the rate of increase is faster at low frequencies than at high frequencies. Slowly, very broad peaks are observed in figure.3,(e) at the x=1.6 sample. This indicates that as the zinc content rises, the activation energy for dielectric relaxation also rises. Because the dielectric loss tangent tan depends on the ability of charges to follow the external applied electric field, the decrease of tan d with increasing frequency is because polarization cannot follow the changes of the external field beyond a certain frequency, as explained above. The increase in

tanσ with increasing temperature is due to an increase in the charge carriers' hopping frequency. In the references [7,28] observed similar behavior.

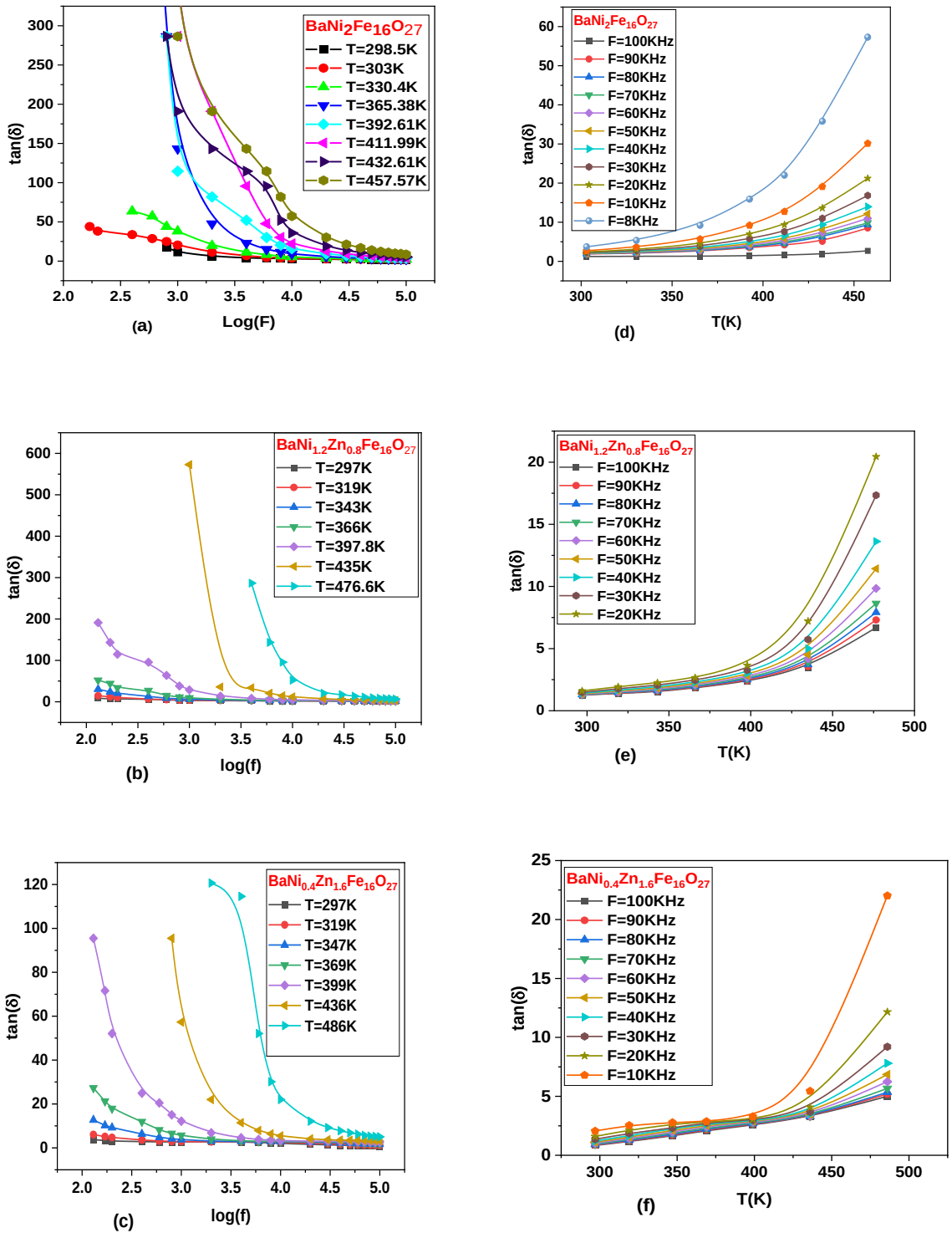

Figure 3. (a,b, c) Frequency dependence (f) of loss tangent tan σ at selected temperature of $BaNi_{2-x}Zn_xFe_{16}O_{27}$ (x=0, 0.8, and1.6); (d, e, f) the temperature dependence of loss tangent with Frequencies.

3.3. Composition dependence.

Figure. 4.a. demonstrates the composition dependence of the real part of the dielectric constant ε′ at room temperature and different frequencies. Figure. 4.b. illustrates the variation of dielectric loss tangent tan σ with composition at room temperature and different frequencies.

It can be seen that the value of a ε′ and tanσ) decreases with increasing Zn^{2+} substitution because of reducing the number of Ni^{2+}–Ni^{3+} ions on the B-sites. This decrease in the hole exchange between Ni^{2+}–Ni^{3+} ions could be due to Zn^{2+} ions preferring the A-sites replacing Ni^{2+} ions that are dispersed nonstatistically in the tetrahedral and octahedral sites. As a result, the value decreases significantly; however, a small amount of Fe^{3+} ions begin to migrate from A-sites to B-sites to compensate for the fall in Ni^{2+} ion concentration at B-sites. The production of Fe^{2+} ions at the B-sites boosts polarization by increasing electron exchange between Fe^{2+}–Fe^{3+} ions [29,30] noticed the same behaviors.

(a) (b)

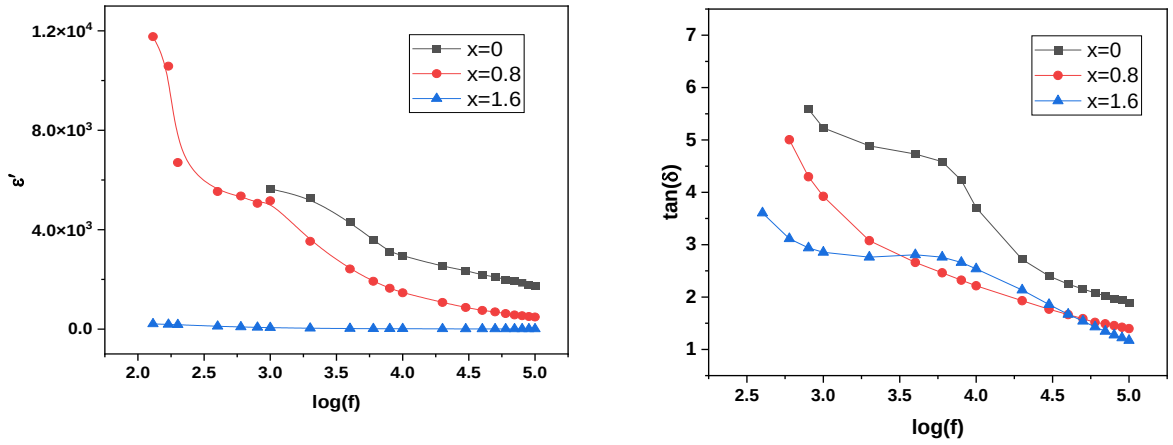

Figure 4. (a) Compositional dependence of (ε′) at room temperature for selected frequencies; (b) Compositional dependence of dielectric loss tangent tan σ at room temperature for selected frequencies.

4. Conclusions

The dielectric constant, the dielectric loss factor tan σ, and dielectric relaxation decrease as the frequency increases. The dielectric constant and dielectric loss increase as the temperature increases. The dielectric constant has abnormally high values and exhibits a dielectric relaxation process or peaks at relatively higher temperatures—the relaxation frequency shifts to a higher frequency as the temperature increases.

The abnormal behavior of the dielectric loss constant ε′′; was observed to shift to lower values as the temperature increases and decreases with increasing frequency and zinc ions. The abnormal behavior was explained by the presence of two types of charge carriers. This has been explained based on the hopping conduction mechanism and the Rezlescu model. The dielectric constant ε‘, dielectric loss tan σ and dielectric relaxation decrease as Zn ion substitution increases. This is explained on the basis ‘that the mechanism of dielectric polarization in ferrites is similar to that of electric conduction and that the displacements of strongly localized electric charge carriers (which increase as Zn ion addition increases) determine the dielectric polarization in ferrites.

Funding

This research received no external funding.

Acknowledgments

This research has no acknowledgment.

Conflicts of Interest

The authors declare no conflict of interest.

References

1. Rana, G.; Dhiman, P.; Kumar, A.; Vo, D.-V.N.; Sharma, G.; Sharma, S.; Naushad, M. Recent Advances on Nickel Nano-Ferrite: A Review on Processing Techniques, Properties and Diverse Applications. *Chemical Engineering Research and Design* **2021**, *175*, 182–208, https://doi.org/10.1016/j.cherd.2021.08.040.
2. Abo El Ata, A.M.; El Nimr, M.K.; El Kony, D.; Al-Hammadi, A.H. Conduction Mechanism of BaCo2−xNixFe16O27. *Journal of Magnetism and Magnetic Materials* **1999**, *202*, 397–404, https://doi.org/10.1016/S0304-8853(99)00387-X.
3. Naiden, E.P.; Maltsev, V.I.; Ryabtsev, G.I. Magnetic Structure and Spin-Orientational Transitions of Hexaferrites of the BaCo2−xZnxFe16O27 System. *phys. stat. sol. (a)* **1990**, *120*, 209–220, https://doi.org/10.1002/pssa.2211200119.
4. Tahir, W.; Khan, M.A.; Gulbadan, S.; Majeed, A.; Mahmood, K. Comprehensive Study of Structural, Physical, and Spectroscopic Properties of Co-Ni Substituted BaMg2Fe16O27 W-Type Hexaferrites. *Journal of Taibah University for Science* **2021**, *15*, 1196–1209, https://doi.org/10.1080/16583655.2022.2025692.
5. Soroka, M.; Buršík, J.; Kužel, R.; Prokleška, J.; Aguirre, M.H. Characterization of W-Type Hexaferrite Thin Films Prepared by Chemical Solution Deposition. *Thin Solid Films* **2021**, *726*, https://doi.org/10.1016/j.tsf.2021.138670.
6. Abo El Ata, A.M.; Ahmed, M.A. Dielectric and AC Conductivity for BaCo2−xCuxFe16O27 Ferrites. *Journal of Magnetism and Magnetic Materials* **2000**, *208*, 27–36, https://doi.org/10.1016/S0304-8853(99)00547-8.
7. Abo El Ata, A.M.; El Nimr, M.K.; El Kony, D.; AL-Hammadi, A.H. Dielectric and Magnetic Permeability Behavior of BaCo2−xNixFe16O27 W-Type Hexaferrites. *Journal of Magnetism and Magnetic Materials* **1999**, *204*, 36–44, https://doi.org/10.1016/S0304-8853(99)00381-9.
8. AL-Hammadi , A.H.; Khoreem , Sadiq H. Investigations on Optical and Electrical Conductivity of Ba/Ni/Zn/Fe16O27 Ferrite Nanoparticles. Biointerface Res Appl Chem 2022, 13, 168, doi:10.33263/BRIAC132.168.
9. Halder, S.; Dey, A.; Sil, S.; Ray, P.P. Study of A.C. Conductivity and Dielectric Behaviour of Hydrothermally Synthesised Molybdenum Disulphide. *J Mater Sci: Mater Electron* **2021**, *32*, 168–181, https://doi.org/10.1007/s10854-020-04749-x.
10. Taneja, S.; Chahar, D.; Thakur, P.; Thakur, A. Influence of Bismuth Doping on Structural, Electrical and Dielectric Properties of Ni–Zn Nanoferrites. *Journal of Alloys and Compounds* **2021**, *859*, https://doi.org/10.1016/j.jallcom.2020.157760.
11. Xi, X.; Chung, D.D.L. Role of Grain Boundaries in the Dielectric Behavior of Graphite. *Carbon* **2021**, *173*, 1003–1019, https://doi.org/10.1016/j.carbon.2020.11.081.
12. Darwish, M.A.; Abosheiasha, H.F.; Morchenko, A.T.; Kostishyn, V.G.; Turchenko, V.A.; Trukhanova, E.L.; Astapovich, K.A.; Trukhanov, A.V. Impact of the Zr-Substitution on Phase Composition, Structure, Magnetic, and Microwave Properties of the BaM Hexaferrite. *Ceramics International* **2021**, *47*, 16752–16761, https://doi.org/10.1016/j.ceramint.2021.02.247.
13. Clausell-Terol, C.; Barba-Juan, A.; Nuño, L. Sintered Microstructure Effect on RF-Wave Shielding Properties of a Cu-Doped Ni–Zn-Polycrystalline Ferrite. *Boletín de la Sociedad Española de Cerámica y Vidrio* **2021**, https://doi.org/10.1016/j.bsecv.2021.09.006.
14. Singh, J.; Singh, C.; Kaur, D.; Narang, S.B.; Jotania, R.B.; Kagdi, A.; Joshi, R.; Bezerra Sombra, A.S.; Zhou, D.; Trukhanov, S.; Panina, L.; Trukhanov, A. Optimization of Performance Parameters of Doped Ferrite-Based Microwave Absorbers: Their Structural, Tunable Reflection Loss, Bandwidth, and Input Impedance Characteristics. *IEEE Transactions on Magnetics* **2021**, *57*, 1–19, https://doi.org/10.1109/TMAG.2021.3063175.
15. Hassan, M.R.; Sarowar Hossain, Md.; Hakim, M.A.; Matin, M.A.; Khan, M.N.I.; Sikder, S.S. Structural Effect on Magneto-Electric Properties in (1-x) BiFe0.9La0.1O3 + XNi0.6Zn0.4Fe1.94V0.06O4 Composites. *Results in Physics* **2021**, *26*, https://doi.org/10.1016/j.rinp.2021.104340.
16. Li, H.; Zhou, Y.; Liu, Y.; Li, L.; Liu, Y.; Wang, Q. Dielectric Polymers for High-Temperature Capacitive Energy Storage. *Chem. Soc. Rev.* **2021**, *50*, 6369–6400, https://doi.org/10.1039/D0CS00765J.
17. Gowtham, B.; Balasubramani, V.; Ramanathan, S.; Ubaidullah, M.; Shaikh, S.F.; Sreedevi, G. Dielectric Relaxation, Electrical Conductivity Measurements, Electric Modulus and Impedance Analysis of WO3 Nanostructures. *Journal of Alloys and Compounds* **2021**, *888*, https://doi.org/10.1016/j.jallcom.2021.161490.

18. Darwish, M.A.; Turchenko, V.A.; Morchenko, A.T.; Kostishyn, V.G.; Timofeev, A.V.; Sayyed, M.I.; Sun, Z.; Podgornaya, S.V.; Trukhanova, E.L.; Kaniukov, E.Y.; Trukhanov, S.V.; Trukhanov, A.V. Heterovalent Substituted BaFe12-XSnxO19 (0.1≤ x ≤1.2) M-Type Hexaferrite: Chemical Composition, Phase Separation, Magnetic Properties and Electrodynamics Features. *Journal of Alloys and Compounds* **2022**, *896*, https://doi.org/10.1016/j.jallcom.2021.163117.
19. Nitika; Rana, A.; Kumar, V. Thermally Stable Ferrous-Doped CoFe2O4 Ferromagnetic Nanoparticles with High Quality Factor for the Use in Electronic Devices. *J Mater Sci: Mater Electron* **2021**, *32*, 18873–18885, https://doi.org/10.1007/s10854-021-06405-4.
20. Iqbal, M.J.; Khan, R.A.; Mizukami, S.; Miyazaki, T. Tailoring of Structural, Electrical and Magnetic Properties of BaCo2 W-Type Hexaferrites by Doping with Zr–Mn Binary Mixtures for Useful Applications. *Journal of Magnetism and Magnetic Materials* **2011**, *323*, 2137–2144, https://doi.org/10.1016/j.jmmm.2011.03.009.
21. Li, C.; Chen, G.; Qiu, X.; Lou, Q.; Gao, X. A Direct Proof for Maxwell–Wagner Effect of Heterogeneous Interface. *AIP Advances* **2021**, *11*, https://doi.org/10.1063/5.0040947.
22. Saengvong, P.; Chanlek, N.; Putasaeng, B.; Pengpad, A.; Harnchana, V.; Krongsuk, S.; Srepusharawoot, P.; Thongbai, P. Significantly Improved Colossal Dielectric Properties and Maxwell—Wagner Relaxation of TiO2—Rich Na1/2Y1/2Cu3Ti4+xO12 Ceramics. *Molecules* **2021**, *26*, https://doi.org/10.3390/molecules26196043.
23. Eman, N.M.; Maruf, H.M.A.R.; Ullah, M.R.; Shirin, N.J.; Hossen, M.B. Dynamic Electric, Dielectric, Impedance, and Modulus Spectroscopy Study with Rietveld Refinement of Al-Substituted NiCuZn Bulk Ceramics. *J Mater Sci: Mater Electron* **2022**, *33*, 1752–1773, https://doi.org/10.1007/s10854-021-07203-8.
24. Narang, S.B.; Singh, A.; Singh, K. High Frequency Dielectric Behavior of Rare Earth Substituted Sr-M Hexaferrite. *Journal of Ceramic Processing Research* **2007**, *8*, 347–351, https://doi.org/10.36410/jcpr.2007.8.5.347.
25. Mangalaraja, R.V.; Manohar, P.; Gnanam, F.D.; Awano, M. Electrical and Magnetic Properties of Ni0.8Zn0.2Fe2O4/Silica Composite Prepared by Sol-Gel Method. *Journal of Materials Science* **2004**, *39*, 2037–2042, https://doi.org/10.1023/B:JMSC.0000017766.07079.80.
26. Kershi, R.M. Redistribution Cations at Sites of Cadmium Ferrite Nanostructures as a Result of Fe2+ and Co2+ Ions Dual Additions and Their Magnetic, Dielectric, Spectroscopic, and Mechanical Properties. *Materials Chemistry and Physics* **2021**, *270*, https://doi.org/10.1016/j.matchemphys.2021.124862.
27. Sathiya Priya, A.; Geetha, D. Structural and Frequency Dependent Dielectric Properties of Ba Doped Ni–Zn Ferrite Powders. *Phosphorus, Sulfur, and Silicon and the Related Elements* **2022**, *197*, 186–191, https://doi.org/10.1080/10426507.2021.2025375.
28. Mazen, S.A.; Nawara, A.S.; Abu-Elsaad, N.I. Investigation of Dielectric Behavior in Ni0.7-XZn0.3MxFe2O4 (M=Mn/Co/Cu) Ferrites by Impedance Spectroscopy. *Ceramics International* **2021**, *47*, 9856–9865, https://doi.org/10.1016/j.ceramint.2020.12.127.
29. Potangale, C.N.; Pardeshi, S.K. Effect of Ni2+ Substitution on DC Electrical Conductivity and Magnetic Properties of Ba1-XNixFe2O4 Synthesized by Citric Acid Gel Method. *Materials Today: Proceedings* **2022**, https://doi.org/10.1016/j.matpr.2021.12.589.
30. Atif, M.; Asghar, M.W.; Nadeem, M.; Khalid, W.; Ali, Z.; Badshah, S. Synthesis and Investigation of Structural, Magnetic and Dielectric Properties of Zinc Substituted Cobalt Ferrites. *Journal of Physics and Chemistry of Solids* **2018**, *123*, 36–42, https://doi.org/10.1016/j.jpcs.2018.07.010.